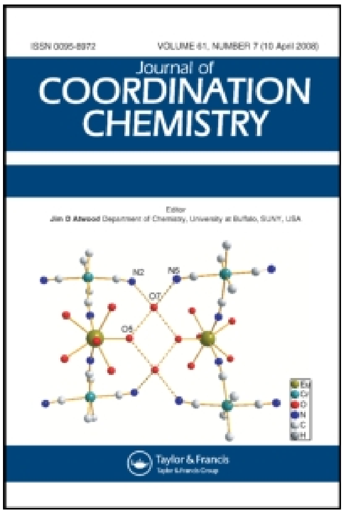

Journal of Coordination Chemistry
Publication details, including instructions for authors and subscription information:
http://www.informaworld.com/smpp/title~content=t713455674

Synthesis, characterization, and catalytic oxidation of ethylbenzene over host (zeolite-Y)/guest (copper(II) complexes of tetraaza macrocyclic ligands) nanocomposite materials

Masoud Salavati-Niasari[ab]; Fatemeh Davar[a]
[a] Institute of Nano Science and Nano Technology, University of Kashan, Kashan, Islamic Republic of Iran [b] Department of Inorganic Chemistry, Faculty of Chemistry, University of Kashan, Kashan, Islamic Republic of Iran

To cite this Article Salavati-Niasari, Masoud and Davar, Fatemeh(2010) 'Synthesis, characterization, and catalytic oxidation of ethylbenzene over host (zeolite-Y)/guest (copper(II) complexes of tetraaza macrocyclic ligands) nanocomposite materials', Journal of Coordination Chemistry, 63: 18, 3240 — 3255, First published on: 19 August 2010 (iFirst)

To link to this Article: DOI: 10.1080/00958972.2010.510557

URL: http://dx.doi.org/10.1080/00958972.2010.510557

Journal of Coordination Chemistry
Vol. 63, No. 18, 20 September 2010, 3240–3255

Taylor & Francis
Taylor & Francis Group

Synthesis, characterization, and catalytic oxidation of ethylbenzene over host (zeolite-Y)/guest (copper(II) complexes of tetraaza macrocyclic ligands) nanocomposite materials

MASOUD SALAVATI-NIASARI*†‡ and FATEMEH DAVAR†

†Institute of Nano Science and Nano Technology, University of
Kashan, P.O. Box 87317-51167, Kashan, Islamic Republic of Iran
‡Department of Inorganic Chemistry, Faculty of Chemistry,
University of Kashan, P.O. Box 87317-51167, Kashan,
Islamic Republic of Iran

(*Received 5 January 2009; in final form 1 June 2010*)

Cu(II) complexes of 14- and 16-membered tetraaza macrocyclic ligands have been encapsulated in nanopores of zeolite-Y by a two-step process in the liquid phase: (1) adsorption of [*bis*(diamine)copper(II)] (diamine = 1,2-diaminoethane, 1,3-diaminopropane, 1,2-diaminobenzene, and 1,3-diaminobenzene); $[Cu(N–N)_2]^{2+}$–NaY; in the nanopores of the zeolite-Y and (2) *in situ* condensation of the copper(II) precursor complex with ethylcinnamate. The new host–guest nanocomposite materials were characterized by chemical analysis and spectroscopic methods. The "neat" and encapsulated complexes exhibit good catalytic activity in the oxidation of ethylbenzene at 333 K, using *tert*-butyl hydroperoxide as the oxidant. Acetophenone was the major product though small amounts of *o*- and *p*-hydroxyacetophenones were also formed revealing that C–H bond activation takes place both at benzylic and aromatic ring carbon atoms.

Keywords: Nanocomposite materials; Copper(II); Tetraaza; Zeolite encapsulation; Oxidation of ethylbenzene

1. Introduction

Studies on the isolation, characterization, and catalytic activity of transition metal complexes encapsulated in various nanoporous materials have received considerable attention because of their specific catalytic applications when compared to homogeneous complexes [1–11]. The heterogenization process provides a rigid framework to the metal complex inside the zeolite due to spatial restrictions, Columbic interactions, and/or covalent bonding. It also facilitates reactions under mild conditions [12]. Encapsulation of metal complexes in nanopores of zeolites alters the redox properties; transition metal complexes encapsulated in various zeolites resemble, to a certain extent, enzymes where the catalytically active centers might be

---

*Corresponding author. Email: salavati@kashanu.ac.ir

Journal of Coordination Chemistry
ISSN 0095-8972 print/ISSN 1029-0389 online © 2010 Taylor & Francis
DOI: 10.1080/00958972.2010.510557

a transition metal ion and the protein sheath provides the stability and steric constraints. Inorganic complexes encapsulated in such constrained environments can therefore be termed as zeozymes [13].

Nanoporous materials are exemplified by crystalline framework solids, such as zeolites, whose crystal structure defines channels and cages i.e., nanopores, of strictly regular dimensions. They can impart shape selectivity for both the reactants and the products in chemical reactions and processes. The large internal surface area and void volumes with extremely narrow pore size distribution as well as functional centers homogeneously dispersed over the surface make nanoporous solids highly active, and there has been a dramatic increase in synthesis, characterization, and application of nanoporous materials [1–16].

In this study, we chose tetraaza ligands and their encapsulated complexes (schemes 1 and 2) in oxidation reactions. Tetraaza copper(II) complexes have not been encapsulated in the nanopores of zeolite-Y and have not been used in oxidation of ethylbenzene. The use of these encapsulated complexes as nanocatalysts can enhance selectivity in the oxidation. The host–guest nanocomposite materials (HGNM) can be windows to selection of a suitable nanocatalyst for oxidation. In this article, we report the synthesis and characterization of copper(II) complexes of 14- and 16-membered tetraaza macrocyclic ligands; [14]aneN_4: 1,5,8,12-tetraaza-2,9-dioxo-4,11-diphenylcyclotetradecane; [16]aneN_4: 1,5,9,13-tetraaza-2,10-dioxo-4,12-diphenylcyclohexadecane; Bzo_2[14]aneN_4: dibenzo-1,5,8,12-tetraaza-2,9-dioxo-4,11-diphenylcyclotetradecane and Bzo_2[16]aneN_4: dibenzo-1,5,9,13-tetraaza-2,10-dioxo-4,12-diphenylcyclohexadecane; and encapsulated within the nanopores of zeolite-Y by template condensation of ethylcinnamate and [*bis*(diamine)copper(II)], $[Cu([14]aneN_4)]^{2+}$–NaY, $[Cu([16]aneN_4)]^{2+}$–NaY, $[Cu(Bzo_2[14]aneN_4)]^{2+}$–NaY, and $[Cu(Bzo_2[16]aneN_4)]^{2+}$–NaY, shown in schemes 1 and 2.

2. Experimental

2.1. *Materials*

2.1.1. Safety note. Copper perchlorate with organic ligands is often explosive and should be handled with caution. All other reagents, solvents, and *tert*-butyl hydroperoxide (TBHP) (50% in ethylene dichloride; 0.42 mL) were purchased from Merck (pro-analysis) and dried using molecular sieves (Linde 4 Å). NaY with the Si : Al ratio of 2.53 was purchased from Aldrich (Lot no. 67812). The complex $[Cu(N–N)_2](ClO_4)_2$ was prepared according to published procedures [17].

2.2. *Physical measurements*

Elemental analysis (carbon, hydrogen, and nitrogen) of the materials was obtained from a Carlo ERBA Model EA 1108 analyzer. X-ray diffraction (XRD) patterns were recorded on a Rigaku D-max C III, X-ray diffractometer using Ni-filtered Cu-Kα radiation. Nitrogen adsorption measurements were performed at 77 K, using a Coulter Ofeisorb 100CX instrument. The samples were degassed at 150°C until a vacuum better

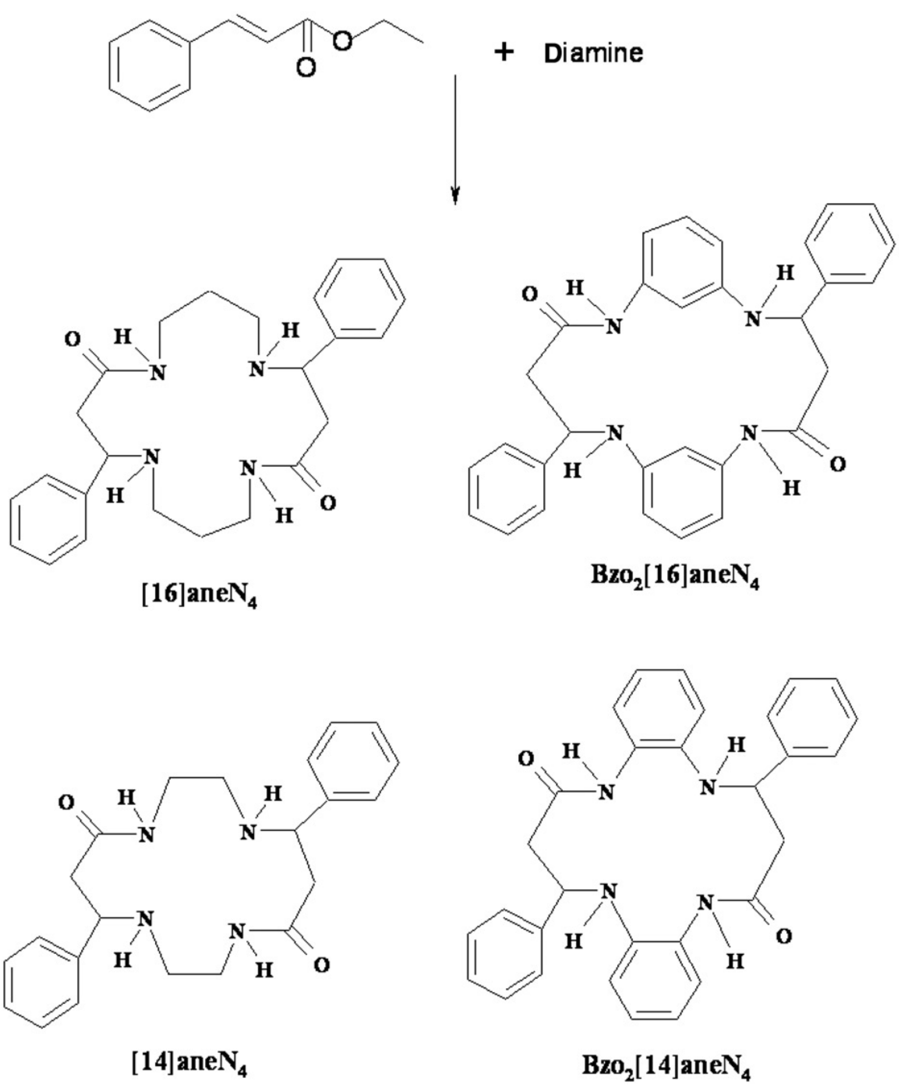

Scheme 1. The 14- and 16-membered tetraaza dioxo diphenyl macrocyclic ligands.

than 10^{-3} Pa was obtained. Micropore volumes were determined by the *t*-method and a "monolayer equivalent area" was calculated from the micropore volume [18, 19]. Electrochemical data were obtained in acetonitrile with $0.1\,\mathrm{mol\,L^{-1}}$ $(n\text{-Bu})_4NClO_4$ as supporting electrolyte. The working electrode was a platinum disc, the auxiliary electrode was a coiled platinum wire, and the reference electrode was $Ag/AgClO_4$ ($0.1\,\mathrm{mol\,L^{-1}}$ in CH_3CN), which showed +0.24 V *versus* SCE. FAB mass spectra were recorded on a Kratos MS50TC spectrometer. FTIR spectra were recorded on a Shimadzu Varian 4300 spectrophotometer in KBr pellets. Electronic spectra of the neat complexes were taken on a Shimadzu UV-Vis scanning spectrometer (Model 2101 PC). The stability of the encapsulated catalyst was checked after the reaction by UV-Vis and possible leaching of the complex was investigated by UV-Vis in the reaction solution

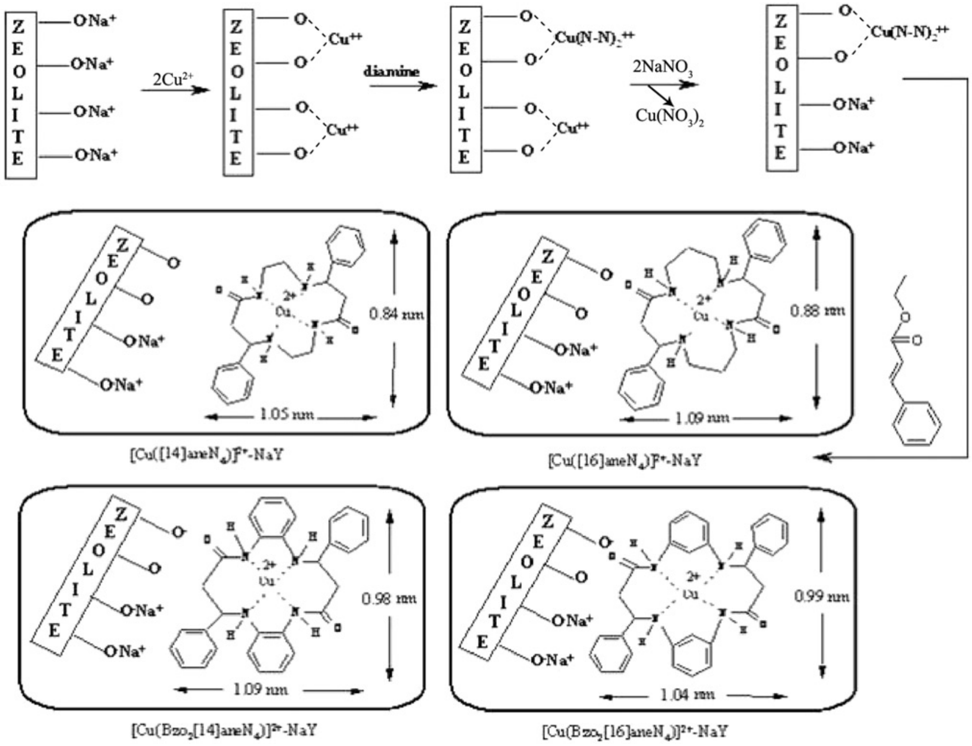

Scheme 2. Encapsulation of copper complexes of the 14- and 16-membered tetraaza dioxo diphenyl macrocycles within the nanopores of zeolite-Y.

after filtration of the zeolite. The amounts of metallocomplexes encapsulated in the zeolite matrix were determined by elemental analysis and by subtracting the amount of metallocomplex left in the solutions after the synthesis of the catalysts as determined by UV-Vis spectroscopy, from the amount taken for the synthesis. Atomic absorption spectra (AAS) were recorded on a Perkin-Elmer 4100–1319 spectrophotometer using a flame approach, after acid (HF) dissolution of known amounts of the zeolitic material and SiO_2 was determined by gravimetric analysis. Diffuse reflectance spectra (DRS) were recorded on a Shimadzu UV/3101 PC spectrophotometer in the range 1500–200 nm, using MgO as reference.

2.3. *Synthesis of 14- and 16-membered tetraaza dioxo diphenyl macrocyclic ligands*

Tetraaza macrocyclic ligands ([14]aneN_4, [16]aneN_4, Bzo_2[14]aneN_4, or Bzo_2[16]aneN_4) were prepared by following the procedures reported [20]. Hot ethanol solution (20 mL) of ethylcinnamate (3.52 g, 0.02 mol) and a hot ethanol solution (20 mL) of diamine (0.02 mol) (1,2-diaminoethane (1.20 g), 1,3-diaminopropane (1.48 g), 1,2-diaminobenzene (2.16 g), and 1,3-diaminobenzene (2.16 g)) were mixed slowly with constant stirring. This mixture was refluxed at 80°C for 12 h with few drops of concentrated HCl. On cooling, a white precipitate was formed, which was filtered, washed with cold ethanol, and dried under vacuum over P_4O_{10}. The purity was checked by HPLC technique. Anal. Calcd for [14]aneN_4: C, 69.4%; H, 7.4%; and N, 14.7%; C/N, 4.7%.

Found: C, 69.3%; H, 7.3%; and N, 14.9%; C/N, 4.7%; νC=O, 1624 cm^{-1}, ν(C–N) + δ(N–H), 1593 cm^{-1}, δ(N–H), 1249 cm^{-1}, ϕ(C=O), 780, and νN–H, 3286. Anal. Calcd for [16]aneN_4: C, 70.6%; H, 7.9%; and N, 13.7%; C/N, 5.1%. Found: C, 70.3%; H, 7.7%; and N, 13.9%; C/N, 5.1%; νC=O, 1620 cm^{-1}, ν(C–N) + δ(N–H), 1590 cm^{-1}, δ(N–H), 1248 cm^{-1}, ϕ(C=O), 780, and νN–H, 3280. Anal. Calcd for Bzo_2[14]aneN_4: C, 75.6%; H, 5.9%; and N, 11.8%; C/N, 6.4%. Found: C, 75.4%; H, 5.7%; N, 11.8%; C/N, 6.4%; νC=O, 1630 cm^{-1}, ν(C–N) + δ(N–H), 1596 cm^{-1}, δ(N–H), 1252 cm^{-1}, ϕ(C=O), 782, and νN–H, 3290. Anal. Calcd for Bzo_2[16]aneN_4: C, 75.6%; H, 5.9%; and N, 11.7%; C/N, 6.5%. Found: C, 75.4%; H, 5.7%; and N, 11.9%; C/N, 6.3%; νC=O, 1627 cm^{-1}, ν(C–N) + δ(N–H), 1594 cm^{-1}, δ(N–H), 1250 cm^{-1}, ϕ(C=O), 782, and νN–H, 3288.

2.4. *Preparation of tetraaza dioxo diphenyl copper(II) complexes*

Copper(II) perchlorate hexahydrate (0.01 mol) dissolved in ethanol (20 mL) was reacted with an ethanol (20 mL) solution of tetraaza ligands ([14]aneN_4, [16]aneN_4, Bzo_2[14]aneN_4, or Bzo_2[16]aneN_4) (0.01 mol) by refluxing for 6 h until an orange solution resulted. The solution was cooled to room temperature and filtered to remove $Cu(OH)_2$. Excess $Li(ClO_4)\cdot 3H_2O$ dissolved in methanol was added to the filtrate, and the mixture was kept in the refrigerator until a red solid was formed. The solids were filtered, washed thoroughly with cold ethanol, and dried in vacuum. Anal. Calcd for [Cu([14]aneN_4)]$(ClO_4)_2$: C, 41.1%; H, 4.4%; N, 8.7%, and Cu, 9.9%; C/N, 4.7%. Found: C, 40.9%; H, 4.2%; N, 8.9%, and Cu, 9.8%; C/N, 4.6%; νC=O, 1620 cm^{-1}, ν(C–N) + δ(N–H), 1591 cm^{-1}, δ(N–H), 1248 cm^{-1}, ϕ(C=O), 779, νN–H, 3258, and νM–N, 470. FAB mass (*m/z*): $[Cu–ClO_4]^+$, 543, $[Cu–2ClO_4]^{2+}$, 444; d ↔ d, 493 (in CH_3CN), and 475 nm (in CH_3NO_2); μ_B, 1.8 B.M; Λ_M, 230 (Ω^{-1} cm^2 (mol L^{-1})$^{-1}$). Anal. Calcd for [Cu([16]aneN_4)]$(ClO_4)_2$: C, 43.0%; H, 4.8%; N, 8.3%, and Cu, 9.5%; C/N, 5.1%. Found: C, 42.7%; H, 4.7%; N, 8.4%; and Cu, 9.3%; C/N, 5.1%; νC=O, 1621 cm^{-1}, ν(C–N) + δ(N–H), 1590 cm^{-1}, δ(N–H), 1247 cm^{-1}, ϕ(C=O), 780, νN–H, 3253, and νM–N, 469. FAB mass (*m/z*): $[Cu–ClO_4]^+$, 571, $[Cu–2ClO_4]^{2+}$, 472; d ↔ d, 496 (in CH_3CN), and 476 nm (in CH_3NO_2); μ_B, 1.8 B.M; Λ_M, 225 (Ω^{-1} cm^2 (mol L^{-1})$^{-1}$). Anal. Calcd for [Cu(Bzo_2[14]aneN_4)]$(ClO_4)_2$: C, 48.8%, H, 3.8%; N, 7.6%, and Cu, 8.6%; C/N, 6.4%. Found: C, 48.6%; H, 3.7%; N, 7.7%; and Cu, 8.5%; C/N, 6.3%; νC=O, 1633 cm^{-1}, ν(C–N) + δ(N–H), 1594 cm^{-1}, δ(N–H), 1251 cm^{-1}, ϕ(C=O), 782, νN–H, 3262, and νM–N, 475. FAB mass (*m/z*): $[Cu–ClO_4]^+$, 639, $[Cu–2ClO_4]^{2+}$, 540; d ↔ d, 490 (in CH_3CN), and 470 nm (in CH_3NO_2); μ_B, 1.8 B.M; Λ_M, 220 (Ω^{-1} cm^2 M^{-1}). Anal. Calcd for [Cu(Bzo_2[16]aneN_4)]$(ClO_4)_2$: C, 48.8%; H, 3.8%; N, 7.6%; and Cu, 8.6%; C/N, 6.4%. Found: C, 48.6%; H, 3.7%; N, 7.7%; and Cu, 8.5%; C/N, 6.3%; νC=O, 1629 cm^{-1}, ν(C–N) + δ(N–H), 1593 cm^{-1}, δ(N–H), 1254 cm^{-1}, ϕ(C=O), 781, νN–H, 3259, and νM–N, 472. FAB mass (*m/z*): $[Cu–ClO_4]^+$, 639, $[Cu–2ClO_4]^{2+}$, 540; d ↔ d, 491 (in CH_3CN), and 473 nm (in CH_3NO_2); μ_B, 1.8 B.M; Λ_M, 218 (Ω^{-1} cm^2 (mol L^{-1})$^{-1}$).

2.5. *Preparation of Cu(II)–NaY*

Two grams of NaY zeolite was suspended in 100 mL of distilled water, which contained $Cu(NO_3)_2\cdot 6H_2O$ (0.025 mol L^{-1}). The mixture was then heated while stirring at 90°C for 24 h. The solid was filtered, washed with hot distilled water till the filtrate was free from any copper(II) (by AAS of filtrate) and dried for 10 h at 80°C under vacuum. The ionic exchange degree was determined by AAS. Anal. Found for NaY: Si, 21.8%; Al, 8.6%; and Na, 7.5%; Si/Al, 2.5%; surface area, 545 $m^2\,g^{-1}$; pore volume, 0.3 $cm^3\,g^{-1}$. Anal. Found for Cu(II)NaY: Si, 21.5%; Al, 8.5%; Na, 3.3%; and Cu, 3.9%; Si/Al, 2.5%; surface area, 532 $m^2\,g^{-1}$; pore volume, 0.3.

2.6. *Preparation of* $[Cu(N–N)_2]^{2+}$*–NaY*

Typically, a 4 g sample of NaY zeolite was mixed with 0.37 g of [*bis*(diamine)copper(II)] perchlorate (diamine = 1,2-diaminopropane, 1,3-diaminopropane, 1,2-diaminobenzene, and 1,3-diaminobenzene) suspended in 100 mL of methanol and refluxed for 8 h. The pale red solid consisting of $[Cu(N–N)_2]^{2+}$ exchanged with Na^+ in NaY and denoted as $[Cu(N–N)_2]^{2+}$–NaY was collected by filtration and washed with ethanol. The resulting zeolites were Soxhlet extracted with DMF (for 4 h) and then with ethanol (for 3 h) to remove excess unreacted diamine and any copper(II) complexes adsorbed onto the external surface of the zeolite crystallines. The resulting light blue solids were dried at 60°C under vacuum for 24 h. Data for $[Cu(N–N)_2]^{2+}$–NaY: surface area, 452 $m^2\,g^{-1}$; pore volume, 0.24 $cm^3\,g^{-1}$.

2.7. *Preparation of HGNM;* $[Cu([14\ or\ 16]aneN_4)]^{2+}$*–NaY and* $[Cu(bzo_2[14\ or\ 16]aneN_4)]^{2+}$*–NaY*

Ethylcinnamate was slowly added to a stirred methanol suspension (100 mL) of $[Cu(N–N)_2]^{2+}$–NaY (2 g) under N_2. The mixture was heated under reflux for 24 h until a pale red suspension resulted. The solution was filtered and the resulting zeolites were Soxhlet extracted with DMF (for 6 h) and then with ethanol (for 5 h) to remove excess unreacted products from amine–ester condensation and any copper(II) complexes adsorbed onto the external surface of the zeolite. The resulting pale red solids were dried at 70°C under vacuum for 12 h. The remaining $[Cu(N–N)_2]^{2+}$ ions in the zeolite were removed by exchanging with aqueous 0.1 mol L^{-1} NaCl solutions. The stability of the encapsulated catalyst was checked after the reaction by UV-Vis; possible leaching of the complex was investigated by UV-Vis in the reaction solution after filtration of the zeolite. The amounts of copper(II) complexes encapsulated in the zeolite matrix were determined by elemental analysis and subtracting the amount of copper(II) complex left from the solutions after the synthesis of the catalysts as determined by UV-Vis spectroscopy, from the amount taken for the synthesis. Anal. Found for $[Cu([14]aneN_4)]^{2+}$–NaY: C, 4.2; H, 1.6; N, 1.0; and Cu, 2.8; C/N, 4.2; Si, 21.1; Al, 8.3; and Na, 5.2; Si/Al, 2.5; νC=O, 1625 cm^{-1}; νN–H, 3256; d ↔ d, 477 nm; surface area, 421 $m^2\,g^{-1}$; pore volume, 0.2 $cm^3\,g^{-1}$. Anal. Found for $[Cu([16]aneN_4)]^{2+}$–NaY: C, 4.3; H, 1.6; N, 0.9; and Cu, 2.8; C/N, 4.8; Si, 21.1; Al, 8.3; and Na, 5.2; Si/Al, 2.5; νC=O, 1623 cm^{-1}; νN–H, 3252; d ↔ d, 479 nm; surface area, 413 $m^2\,g^{-1}$; pore volume, 0.2 $cm^3\,g^{-1}$. Anal. Found for $[Cu(Bzo_2[14]aneN_4)]^{2+}$–NaY: C, 4.3; H, 1.6; N, 0.7; and Cu, 2.7; C/N, 6.2; Si, 21.0; Al, 8.3; and Na, 5.2; Si/Al, 2.5; νC=O, 1633 cm^{-1}; νN–H, 3260; d ↔ d, 473 nm; surface area, 374 $m^2\,g^{-1}$; pore volume, 0.1 $cm^3\,g^{-1}$. Anal. Found for $[Cu(Bzo_2[16]aneN_4)]^{2+}$–NaY: C, 4.3; H, 1.6; N, 0.7; and Cu, 2.7; C/N, 6.2; Si, 21.0;

Al, 8.3; and Na, 5.2; Si/Al, 2.5; νC=O, 1630 cm^{-1}; νN–H, 3260; d ↔ d, 475 nm; surface area, 361 $m^2 g^{-1}$; pore volume, 0.1 $cm^3 g^{-1}$.

2.8. *Oxidation of ethylbenzene; general procedure*

The catalytic activities were conducted in a 25 mL round-bottom glass flask, placed in a thermostated oil bath and fitted with a water cooled condenser. In a typical oxidation, ethylbenzene (0.106 g, 1 mmol), catalyst (0.004 mmol in case of "neat" complexes and 0.004 mmol in case of HGNM), TBHP (50% in ethylene dichloride; 0.42 mL), and CH_3CN (1 mL) were taken and the reaction was conducted at 333 K for 10 h under Ar. The progress of the reaction was monitored by HPLC and the products were identified by GC–MS.

3. Results and discussion

3.1. *Synthesis and characterization of HGNM*

The C, H, and N analyses of the neat copper complexes showed close similar theoretical values. The molecular formulae of the tetraaza complexes have been assigned on the basis of their elemental analysis. Preliminary identification of the metal complexes was made on the basis of their IR spectra, which exhibited no bands characteristic of free primary amine, supporting the proposed macrocyclic skeleton (scheme 1). The copper contents of the HGNM catalysts were estimated by dissolving known amounts of the catalyst in concentrated HCl and from these solutions, the copper content was estimated by using AAS. The chemical compositions confirmed the purity and stoichiometry of the neat and encapsulated complexes. The chemical analyses of the samples revealed the presence of organic matter with a C/N ratio similar to that for neat complexes. The molar ratio of Si/Al obtained by chemical analysis for zeolites Cu(II)–NaY and the zeolite complexes were almost in the same ratio, indicating little change in the zeolite framework due to de-alumination in metal ion exchange. The parent NaY zeolite has Si/Al molar ratio of 2.53, which corresponds to a unit cell formula $[Na_{56}[(AlO_2)_{56}(SiO_2)_{136}]$. The unit cell formula of metal-exchanged zeolites showed a copper dispersion of 10.8 mol per unit cell $[(Na_{33.8}Cu_{10.8}[(AlO_2)_{56}(SiO_2)_{136}]\cdot nH_2O)$. The analytical data of each complex indicated Cu : C : N molar ratios close to those calculated for the mononuclear structure. However, traces of free $[Cu(N–N)_2]^{2+}$ in the lattice are higher than the stoichiometric requirement, and only a small amount of $[Cu(N–N)_2]^{2+}$ has undergone complexation in exchange with zeolite and the rest is expected to be removed through re-exchange with NaCl solution.

Synthesis of tetraaza copper(II) complexes encapsulated in the nanocavity of zeolite-Y involves exchange of $[Cu(N–N)_2]^{2+}$ (diamine = 1,2-diaminopropane, 1,3-diaminopropane, 1,2-diaminobenzene, and 1,3-diaminobenzene) with NaY in methanol solution and reaction of $[Cu(N–N)_2]^{2+}$–NaY with excess ethylcinnamate in methanol where ethylcinnamate slowly enters into the nanocavity of zeolite-Y due to its template nature and interacts with $[Cu(N–N)_2]^{2+}$. Soxhlet extraction using methanol finally purified the impure complexes. The remaining free metal ions in zeolite were removed by exchanging with aqueous 0.01 mol L^{-1} NaCl solution. Thus, the formula of copper(II) complex may be written as $[Cu([14]aneN_4)]^{2+}$–NaY, $[Cu([16]aneN_4)]^{2+}$–NaY, $[Cu(Bzo_2[14]aneN_4)]^{2+}$–NaY, and $[Cu(Bzo_2[16]aneN_4)]^{2+}$–NaY. The percentage of metal was determined before and after encapsulation by inductively coupled plasma (ICP). After extraction with methanol, the metal ion content found after encapsulation is only due to the presence of metal complexes in supercages of the zeolite-Y. The molecular formula of the complexes are based on the neat complexes $[Cu([14]aneN_4)]^{2+}$, $[Cu([16]aneN_4)]^{2+}$, $[Cu(Bzo_2[14]aneN_4)]^{2+}$, and $[Cu(Bzo_2[16]aneN_4)]^{2+}$ that have also been prepared and characterized.

XRD patterns of encapsulated complexes are shown in figure 1. These complexes exhibit similar peaks to those of zeolite-Y; except for a slight change in the intensity of the peaks, no new crystalline pattern emerges, confirming that the framework and crystallinity of the zeolite were not destroyed during the preparation, and that the complexes were distributed in the cages. The relative peak intensities of the 220, 311, and 331 reflections are correlated with the locations of cations. In zeolite-Y, the order of peak intensity is in the order $I_{331} \gg I_{220} > I_{311}$, while in encapsulated complexes, the order of peak intensity became $I_{331} \gg I_{311} > I_{220}$. The difference indicates that the ion-exchanged Cu^{2+}, which substitutes at the location of Na^+, undergoes rearrangement during complexation.

The surface areas and pore volumes of the catalysts were measured. The encapsulation of $[Cu([14]aneN_4)]^{2+}$–NaY, $[Cu([16]aneN_4)]^{2+}$–NaY, $[Cu(Bzo_2[14]aneN_4)]^{2+}$–NaY,

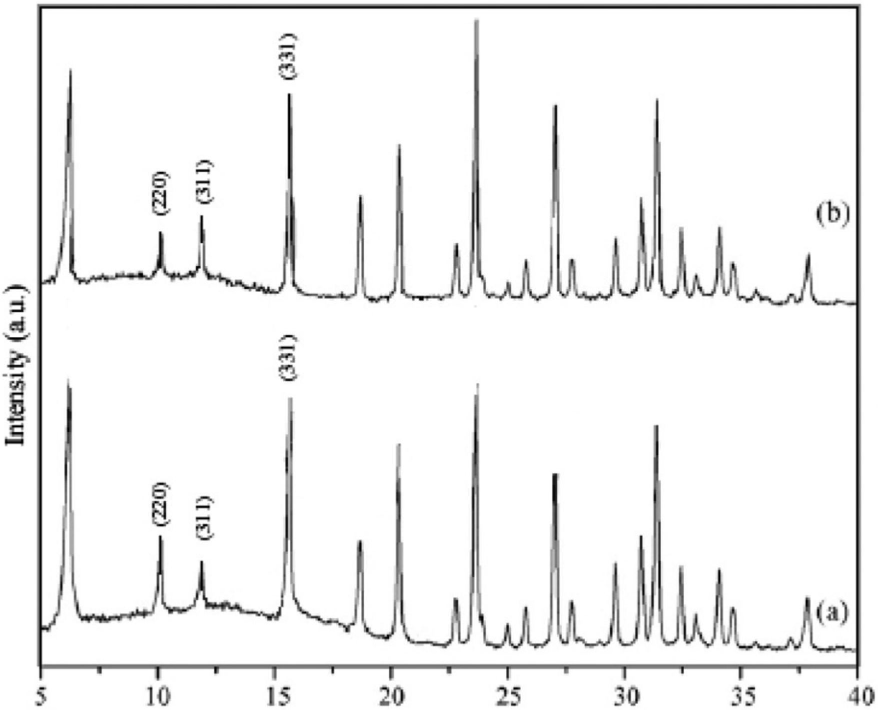

Figure 1. X-ray diffractograms of (a) zeolite-Y and (b) $[Cu([14]aneN_4)]^{2+}$–NaY.

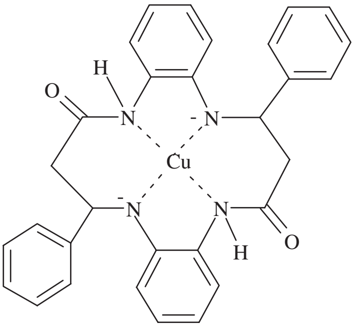

Scheme 3. Deprotonation of $[Cu(Bzo_2[14]aneN_4)]$ in the presence of amine base.

and $[Cu(Bzo_2[16]aneN_4)]^{2+}$–NaY complexes in zeolite reduced the adsorption capacity and the surface area of the zeolite. The lowering of the pore volume and surface area indicated the presence of $(Cu([14]aneN_4)]^{2+}$, $[Cu([16]aneN_4)]^{2+}$, $[Cu(Bzo_2[14]aneN_4)]^{2+}$, and $[Cu(Bzo_2[16]aneN_4)]^{2+})$ within the zeolite nanocages and not on the external surface.

3.2. *Synthesis and characterization of "neat" complexes*

The molecular formulae of the complexes have been assigned on the basis of their elemental analyses and the molecular ion peaks in the mass spectra. All mass spectra showed molecular ion peaks for the 1 : 1 metal-to-ligand stoichiometry with no further peaks above them. A preliminary identification of the metal complexes was made on the basis of their IR spectra, which exhibited no characteristic bands of free primary amine, thus supporting the proposed macrocyclic skeleton (scheme 1). The deep red complexes "$[Cu([14 \text{ or } 16]aneN_4)](ClO_4)_2$ and $[Cu(Bzo_2[14 \text{ or } 16]aneN_4)](ClO_4)_2$" readily dissolve in polar solvents, such as H_2O, CH_3CN, CH_3NO_2, and $(CH_3)_2SO_2$. The copper(II) complexes are extremely stable in the solid state and in solution and are relatively stable against ligand dissociation even in highly acidic solutions. The molar conductance values of the complexes ($218–230\,\Omega^{-1}\,mol^{-1}\,cm^2$) as measured in CH_3NO_2 correspond to 1 : 2 electrolytes. The overall geometries of all macrocycles have been deduced on the basis of the observed values of the magnetic moments and the band positions in the electronic spectra. The magnetic moments ($1.80–1.85\,\mu_B$) of the Cu(II) complexes measured in the solid state correspond to square planar geometry.

The 14- and 16-membered tetraaza macrocyclic copper(II) complexes undergo intense color changes due to deprotonation of the macrocyclic ligand in the presence of amine bases, such as C_5H_5N and Et_3N (Scheme 3). Similar N–H deprotonations have been observed with other metal complexes containing N–H linkages. For the copper(II) complex, Et_3N is sufficiently basic to facilitate formation of the molecular complex. For the preparation of the deprotonated form of $[Cu(Bzo_2[14]aneN_4)](ClO_4)_2$, Et_3N (0.5 mL) was added to a deaerated solution of 200 mg of $[Cu(Bzo_2[14]aneN_4)](ClO_4)_2$ in 15 mL of CH_3CN. The shiny brown product, which began precipitating within minutes, was filtered after 0.5 h under an N_2 atmosphere, washed with anhydrous ethanol, and dried in vacuum. IR (KBr, cm^{-1}): 3215 ($\nu_{N–H}$). $[Cu(C_{30}H_{26}N_4)]$: Found: Cu, 11.7%; C, 66.8%; H, 4.8%; and N, 10.5%. Calcd: Cu, 11.8%; C, 67.0%; H, 4.9%; and N, 10.4%. The N–H stretching frequency of this compound $[Cu(C_{30}H_{26}N_4)]$, 3215 cm^{-1}, is reduced significantly from its dicationic precursor, $[Cu(Bzo_2[14]aneN_4)](ClO_4)_2$, $3262\,cm^{-1}$.

IR spectrum of the ligand does not exhibit any band for the free primary diamine and hydroxyl group. The absorptions of tetraaza at 730–770 and $1415–1645\,cm^{-1}$ [21] are due to the phenyl. Four new bands present in the spectrum of the free ligand in the regions ~1620, ~1590, ~1248, and $\sim780\,cm^{-1}$ correspond to amide I [ν(C=O)], amide II [ν(C–N) + δ(N–H)], amide III [δ(N–H)], and amide IV [φ(C=O)] bands, respectively [22]. A sharp band at $\sim3287\,cm^{-1}$ may be due to [ν(N–H)] of the secondary amino group [23]. The IR spectra of all the complexes showed a single sharp absorption around $\sim3250\,cm^{-1}$ which may arise from a secondary amine, $\nu_{N–H}$, although its position is lower by $\sim30\,cm^{-1}$ than the analogous metal-free tetraaza ligands [24–27]. This suggests that the secondary amine nitrogens coordinate confirmed by the appearance of $\nu_{M–N}$ bands at $340–350\,cm^{-1}$ in the complexes. The IR bands of all encapsulated complexes are weak in comparison with the neat complexes due to their low concentrations in zeolite nanocages. The four entrapped complexes exhibit very similar IR spectra with bands at all regions that are shifted $\sim2\,cm^{-1}$ relative to those of the corresponding free complexes.

Copper(II) complexes with 14- and 16-membered tetraaza macrocyclic ligands "$[14]aneN_4$; $[16]aneN_4$; $Bzo_2[14]aneN_4$; $Bzo_2[16]aneN_4$" exist in aqueous solution as an equilibrium mixture of a red square planar and a green octahedral species. Solution of tetraaza macrocyclic copper(II) complexes in coordinating solvents (such as H_2O, CH_3CN, etc.) show an absorption maximum at ~470 nm, characteristic for square planar red species and at ~490 nm, characteristic for green octahedral species [24–28]. As shown above, the molar absorption coefficient of the ligand field transition band for complexes measured in H_2O or CH_3CN is smaller than that in CH_3NO_2, a non-coordinating solvent. This result is quite similar to those reported for other related polyaza macrocyclic complexes, indicating that the complex dissolves in H_2O or CH_3CN to produce an equilibrium mixture of square planar $[Cu(Bzo_2[14]aneN_4)]^{2+}$ and octahedral *trans*-$[Cu(Bzo_2[14]aneN_4)(solvent)_2]^{2+}$ (solvent = H_2O or CH_3CN) [24–37]. The 14- and 16-membered tetraaza and some tetraaza macrocyclic Cu(II) complexes exist in water as equilibrium mixture of red square planar $[Cu(Bzo_2[14]aneN_4)]^{2+}$ and green octahedral $[Cu(Bzo_2[14]aneN_4)(H_2O)_2]^{2+}$. The electronic spectra of copper(II) complexes are comparable to other similar saturated tetraaza macrocyclic square planar copper(II) complexes, indicating that the tetraaza ligands of this study do not differ significantly from the tetraaza ligands with respect to ligand field strength [24–37].

The UV-Vis data of "neat" and zeolite-Y encapsulated complexes are shown in figure 2. The "neat" complexes in $MeNO_2$ showed a characteristic UV band of ligand origin at 470–500 nm. A weak band due to copper-centered d ↔ d transitions was observed in the visible range at ~490 nm. The size of the macrocyclic ligand affected the structure. As a consequence of this, the d ↔ d band shifted from 490 nm in $[Cu(Bzo_2[14]aneN_4)](ClO_4)_2$ to 491 nm in $[Cu(Bzo_2[16]aneN_4)](ClO_4)$. This shift in the band position to higher energy indicates that the 14-membered tetraaza ligands provide greater stability than the 16-membered tetraaza ligands and the ligand field is stronger in 14-membered than in 16-membered complexes. When the complexes were encapsulated in zeolite-Y, the d ↔ d band shifted again to the higher energy side. The stability of the complexes apparently increases when they are encapsulated in zeolite-Y. The position of the d ↔ d band corresponds to square planar geometry for tetraaza macrocyclic copper(II) complexes [38].

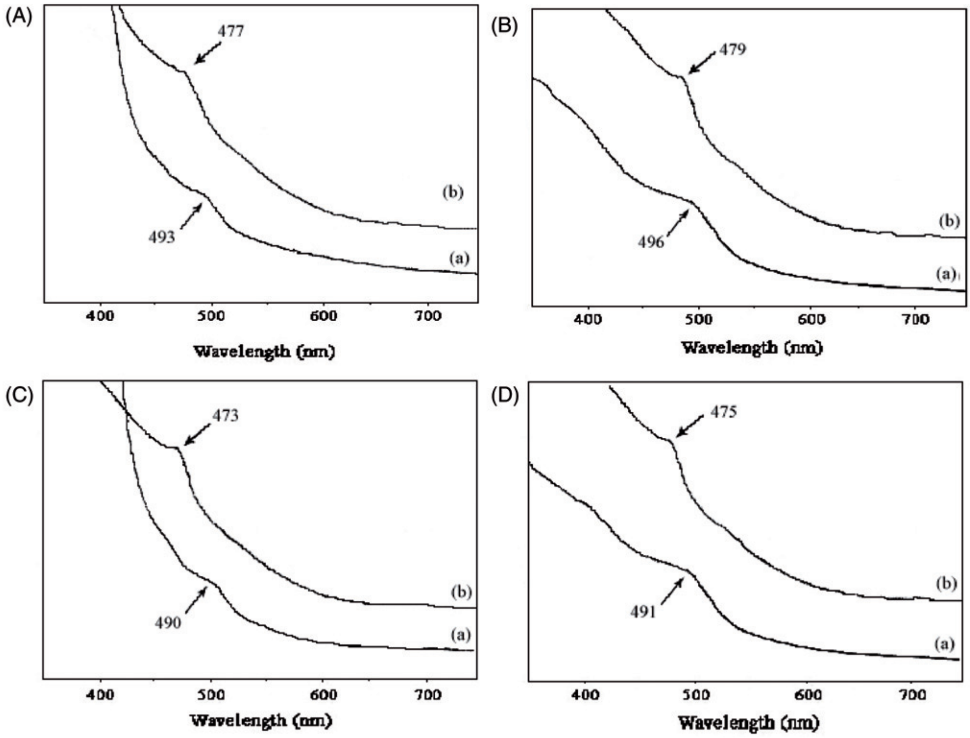

Figure 2. UV-Vis and DRS spectra of (A): (a) $[Cu([14]aneN_4)](ClO_4)_2$, (b) $[Cu([14]aneN_4)]^{2+}$–NaY; (B): (a) $[Cu([16]aneN_4)](ClO_4)_2$, (b) $[Cu([16]aneN_4)]^{2+}$–NaY; (C): (a) $[Cu(Bzo_2[14]aneN_4)](ClO_4)_2$, (b) $[Cu(Bzo_2[14]aneN_4)]^{2+}$–NaY; and (D): (a) $[Cu(Bzo_2[16]aneN_4)](ClO_4)_2$, (b) $[Cu(Bzo_2[16]aneN_4)]^{2+}$–NaY.

Cyclic voltammetric data are summarized in table 1. Table 1 shows that oxidation and reduction potentials of the copper(II) complexes of the tetraaza copper(II) complexes do not differ significantly from other $[14]aneN_4$ complexes. This suggests that macrocycles have Lewis basicities and hole size similar to those of the $[14]aneN_4$ in spite of the structural differences. A pronounced shift in oxidation state stability occurs when there is a change in macrocyclic ring size. An increase in ring size promotes formation of Cu(I), while rendering the oxidation to copper(III) more difficult. The difference between the $[Cu([14]aneN_4)]^{2+}$ and $[Cu((CH_3)_6[16]1,4,12\text{-}trieneN_4)]^{2+}$ complexes amounts to 0.3 V. Busch *et al.* [39] suggested that this difference is primarily due to deviations from the ideal metal donor distances accompanying the redox changes. This concept of optimum fit between the coordinated metal ion and the "hole size" provided by the macrocyclic ligand is also in accord with theoretical conclusions and electronic spectroscopic studies. The more common effect of ligand unsaturation also favors the formation of the lower valent states of the complexes and causes the copper(II) to copper(III) process to occur at higher energy. The effect of the Bzo function on the reduction reactions of the copper macrocycles is very pronounced and structures containing this moiety form stable complexes in lower valence states at relatively mild potentials [40–43].

Table 1. Cyclic voltammetric data for copper(II) complexes with 14- and 16-membered tetraaza macrocycles.[a,b]

Complexes	Oxidation potential (*V*), $[Cu(polyaza)]^{2+}$/ $[Cu(polyaza)]^{3+}$	Reduction potential (*V*) $[Cu(polyaza)]^{2+}$/ $[Cu(polyaza)]^{+}$	References
$[Cu(Bzo_2[14]aneN_4)](ClO_4)_2$	1.34	−1.09	This study
$[Cu([14]aneN_4)](ClO_4)_2$	1.36	−1.07	This study
$[Cu([16]aneN_4)](ClO_4)_2$	1.40	−1.05	This study
$[Cu(Bzo_2[16]aneN_4)](ClO_4)_2$	1.41	−1.04	This study
$[Cu(H_2Bzo_2[14]aneN_6)](ClO_4)_2$	1.52	−1.08	[39]
$[Cu((CH_3)_2Bzo_2[14]aneN_6)](ClO_4)_2$	1.53	−1.07	[39]
$[Cu(Et_2Bzo_2[14]aneN_6)](ClO_4)_2$	1.54	−1.06	[39]
$[Cu(Bu_2Bzo_2[14]aneN_6)](ClO_4)_2$	1.55	−1.03	[39]
$[Cu((Allyl)_2Bzo_2[14]aneN_6)](ClO_4)_2$	1.55	−1.03	[39]
$[Cu((Benzyl)_2Bzo_2[14]aneN_6)](ClO_4)_2$	1.49	−1.11	[39]
$[Cu((CH_3)_2Bzo_2[14]aneN_6)](ClO_4)_2$	1.31	−1.14	[40]
$[Cu((Et_2[14]aneN_6)](ClO_4)_2$	1.32	−1.07	[40]
$[Cu([14]aneN_4)](ClO_4)_2$	1.35	−1.10	[41]
$[Cu((CH_3)_2[16]aneN_6)](ClO_4)_2$	1.43	−1.03	[42]
$[Cu(Et_2[16]aneN_6)](ClO_4)_2$	1.42	−1.01	[42]

[a] Measured in acetonitrile solutions; 0.1 mol L^{-1} $(n\text{-}Bu)_4NClO_4$ *vs.* SCE.

[b] Redox potential of this study and Ref. [38] were measured against a Ag/Ag^+ (0.1 mol L^{-1}) reference electrode and converted to the values measured against the SCE by adding +0.24 V.

3.3. *Catalytic activity*

The N_4-macrocyclic copper(II) complexes exhibited good activity in oxidation of ethylbenzene using TBHP (table 2). Blank reactions performed over NaY zeolite under identical conditions show only negligible conversion, indicating that zeolite host is inactive for oxidation. Furthermore, TBHP alone is unable to oxidize the substrates in the absence of any catalyst. Also, no reaction occurred when aqueous hydrogen peroxide was used in place of TBHP, as the oxidant. In representative tests, zeolite complex was filtered out and the filtrate was analyzed for copper content using AAS. The absence of metal ions in solution phase indicates that no leaching of complexes has occurred during reaction, as they are intact in the pores. These observations suggest that the oxidations occur due to the catalytic nature of the encapsulated tetraaza macrocyclic complexes, and no significant role is played by either the zeolite support or free complexes.

Acetophenone is the major product; *o*-/*p*-hydroxyacetophenones and other products, such as benzaldehyde are also formed in small quantities (table 3). The activity of Cu(II)–NaY catalyst has also been included in table 3 to compare the effect of the ligand on the activity of catalyst. Increase of conversion percentage from 31.4% to 50.3% comparing Cu(II)–Y with $[Cu(Bzo_2[14]aneN_4)]^{2+}$–NaY indicates that the ligand has increased the activity of catalyst by a factor of 1.6. From the results indicated in tables 2 and 3, it is evident that acetophenone has been formed selectively in the presence of all catalysts. The trend observed in tables 2 and 3 can be explained by the donor ability of ligand available in the complex catalysts. The type of the tetraaza macrocyclic ring and encapsulation affected the activity and product selectivity. Conversion for copper(II) complexes with different tetraaza dioxo diphenyl macrocyclic

Table 2. Oxidation of ethylbenzene with TBHP catalyzed by copper(II) complexes.[a]

Catalyst	Conversion (%)	Selectivity (%) Acetophenone	*o*-/*p*-Hydroxyacetophenone	Other products
$[Cu([14]aneN_4)](ClO_4)_2$	58.6	83.4	15.2	1.4
$[Cu([16]aneN_4)](ClO_4)_2$	51.7	80.4	17.4	2.2
$[Cu(Bzo_2[14]aneN_4)](ClO_4)_2$	62.4	89.7	8.3	2.0
$[Cu(Bzo_2[14]aneN_4)](ClO_4)_2$[b]	41.5	92.3	6.3	1.4
$[Cu(Bzo_2[14]aneN_4)](ClO_4)_2$[c]	59.7	87.4	11.3	1.3
$[Cu(Bzo_2[14]aneN_4)](ClO_4)_2$[d]	38.2	80.2	18.6	1.2
$[Cu(Bzo_2[16]aneN_4)](ClO_4)_2$	47.3	86.2	12.4	1.4

[a] Reaction conditions: ethylbenzene, 0.105 g (1 mmol); catalyst, 0.004 mmol; 50% TBHP in ethylenedichloride, 0.42 mL; CH_3CN, 1 mL; temperature, 333 K; and time, 10 h.
[b] Catalyst, 0.002 mmol.
[c] Catalyst, 0.006 mmol
[d] Catalyst, 0.008 mmol.

Table 3. Oxidation of ethylbenzene with TBHP catalyzed by HGNM.[a]

Catalyst	Conversion (%)	Selectivity (%) Acetophenone	*o*-/*p*-Hydroxyacetophenone	Other products
$[Cu([14]aneN_4)]^{2+}$–NaY	46.1	90.7	4.9	4.4
$[Cu([16]aneN_4)]^{2+}$–NaY	40.2	93.6	4.2	2.2
$[Cu(Bzo_2[14]aneN_4)]^{2+}$–NaY	50.3	97.3	2.7	–
$[Cu(Bzo_2[14]aneN_4)]^{2+}$–NaY[b]	49.7	96.5	3.5	–
$[Cu(Bzo_2[14]aneN_4)]^{2+}$–NaY[c]	49.1	96.1	3.9	–
$[Cu(Bzo_2[14]aneN_4)]^{2+}$–NaY[d]	48.3	95.0	5.0	–
$[Cu(Bzo_2[16]aneN_4)]^{2+}$–NaY	36.4	96.4	3.6	–
Cu^{2+}–NaY	31.4	62.7	3.2	34.1

[a] Reaction conditions: ethylbenzene, 0.105 g (1 mmol); catalyst, 0.004 mmol; 50% TBHP in ethylenedichloride, 0.42 mL; CH_3CN, 1 mL; temperature, 333 K; and time, 10 h.
[b] First reuse.
[c] Second reuse.
[d] Third reuse.

ligands decreased in the order: $Bzo_2[14]aneN_4 > [14]aneN_4 > [16]aneN_4 > Bzo_2[16]aneN_4$ (for "neat" and encapsulated complexes). The encapsulated complexes exhibited lower activity than the "neat" complexes.

Homogeneous catalysts are prone to deactivation by dimerization of active centers, which is expected to be reduced by encapsulating them in zeolites. Comparing between "neat complexes" and HGNM as catalysts provides evidence that "neat complexes" gave higher conversion of ethylbenzene than their corresponding HGNM. For homogeneously catalyzed reactions, the termination of catalytic cycle may occur because of two factors, formation of Cu–O–Cu species, which has poor catalytic activity, or due to oxidative degradation of metal complexes. $[Cu(Bzo_2[14]aneN_4)]^{2+}$–NaY was recyclable for oxidation of ethylbenzene with TBHP to establish the effect of encapsulation on stability. The initial run shows a conversion of 50.3% and it is only marginally reduced to 49.7% on recycling the catalyst. These results indicate that

Table 4. Comparing catalytic activity of encapsulated tetraaza copper(II) complexes between this and other study.

Catalyst	Conversion (%)	Selectivity (%)			References
		Acetophenone	o-/p-Hydroxyacetophenone	Other products	
$[Cu(Bzo_2[14]aneN_4)]^{2+}$–NaY	50.3	97.3	2.7	–	This study
$[Cu([H]_2–N_4)]^{2+}$–NaY	58.2	96.4	3.6	–	[43]
$[Cu(cyclen)^a]^{2+}$–NaY	30.5	80.2	4.3	15.5	[45]
$[Cu(Me_4cyclen)^b]^{2+}$–NaY	27.8	85.9	6.3	7.8	[45]
$[Cu(cyclam)^c]^{2+}$–NaY	44.4	98.0	2.0	–	[45]

[a] Cyclen, 1,4,7,10-tetraazacyclononane.
[b] Me_4cyclen, 1,4,7,10-tetramethyl-1,4,7,10-tetraazacyclodecane.
[c] Cyclam, 1,4,8,11-tetrazacyclotetradecane.

$[Cu(Bzo_2[14]aneN_4)]^{2+}$–NaY complex is more recyclable than the neat complex for oxidation of ethylbenzene without much loss in activity. Thus, encapsulation of complexes in zeolites increases the life of the catalyst by reducing dimerization due to the restriction of internal framework structure. IR spectrum of the recycled sample is quite similar to that of fresh sample, indicating little changes in the coordination of $Bzo_2[14]aneN_4$ after the oxidation reactions.

The results clearly suggest that $[Cu(Bzo_2[14]aneN_4)]^{2+}$–NaY are efficient catalysts for the conversion of ethylbenzene to acetophenone with 97.3% selectivity. Comparison of catalytic activity between encapsulated tetraaza copper(II) complexes in this study and similar studies is shown in table 4. In 2005, when $[Cu([H]_2–N_4)]^{2+}$–NaY was applied as a catalyst [43], reaction selectivity for acetophenone as a major product decreases about 1% compared with $[Cu(Bzo_2[14]aneN_4)]^{2+}$–NaY; however, the conversion increases to about 8%. In other literature [44], when $[Cu([H]_2–N_4)]^{2+}$–NaY and $[Cu(Me_4cyclen)^b]^{2+}$–NaY were used as catalysts, selectivity and conversion decreased. In addition, these reactions contained by-products while there were no other products except acetophenone and hydroxyacetophenone. Also, $[Cu(cyclam)^c]^{2+}$–NaY was applied as a catalyst in the literature and the results showed decreased conversion and increased selectivity. More activity of the $Bzo_2[14]aneN_4$ system arises from the electron-donating ligand which facilitates the electron transfer rate, a process previously observed by us in other oxidation reactions [45, 46]. All conversions in this study show a higher selectivity when compared to that obtained using metal containing porous and nonporous materials.

4. Conclusion

In summary, Cu(II) complexes of 14- and 16-membered tetraaza macrocyclic complexes have been encapsulated in the nanopores of zeolite-Y. The neat and encapsulated copper complexes of 14- and 16-membered tetraaza dioxo diphenyl macrocycles within the nanopores of zeolite-Y exhibited good catalytic activity in the oxidation of ethylbenzene, using TBHP as an oxidant. The results clearly suggest that $[Cu(Bzo_2[14]aneN_4)]^{2+}$–NaY is efficient for conversion of ethylbenzene to acetophenone with 97.3% selectivity. The encapsulated complexes exhibit enhanced stability and selectivity in the oxidation reaction. These encapsulated systems offer structural integrity by having a uniform distribution of the metal complex in the pore structure of the support. The zeolite framework keeps the guest complexes dispersed and prevents their dimerization, leading to retention of catalytic activity. Future research on this system is expected to explore its industrial applications for partial oxidation reactions.

Acknowledgment

The author is grateful to the Council of University of Kashan for providing financial support to undertake this research.

References

[1] N. Herron. *J. Coord. Chem.*, **19**, 25 (1988).

[2] I.W.C.E. Arends, R.A. Sheldon. *Appl. Catal., A*, **212**, 175 (2001).

[3] (a) M.R. Maurya, S.J.J. Titinchi, S. Chand. *J. Mol. Catal. A: Chem.*, **214**, 257 (2004); (b) M. Salavati-Niasari. *J. Mol. Catal. A: Chem.*, **284**, 97 (2008); (c) M. Salavati-Niasari, A. Sobhani. *J. Mol. Catal. A: Chem.*, **285**, 58 (2008).

[4] D.E. de Vos, P.P. Knops-Gerrits, D.L. Vanoppen, P.A. Jacobs. *Supramol. Chem.*, **6**, 49 (1995).

[5] (a) P.P. Knops-Gerrits, D.E. de Vos, P.A. Jacobs. *J. Mol. Catal. A: Chem.*, **117**, 57 (1997); (b) M. Salavati-Niasari. *Microporous Mesoporous Mater.*, **92**, 173 (2006); (c) M. Salavati-Niasari. *Microporous Mesoporous Mater.*, **95**, 248 (2006).

[6] M. Salavati-Niasari. *Chem. Lett.*, **34**, 244 (2005).

[7] M. Salavati-Niasari. *Chem. Lett.*, **34**, 1444 (2005).

[8] M.L. Kantam, K.V.S. Ranganath, M. Sateesh, K.B.S. Kumar, B. Manoranjan. *J. Mol. Catal. A: Chem.*, **225**, 15 (2005).

[9] C. Hardacre, S.P. Katdare, D. Milroy, P. Nancarrow, D.W. Rooney, J.M. Thompson. *J. Catal.*, **227**, 44 (2004).

[10] V.R. Choudhary, S.K. Jana, N.S. Patil, S.K. Bhargava. *Microporous Mesoporous Mater.*, **57**, 21 (2003).

[11] (a) D. Srinivas, S. Sivasanker. *Catal. Surv. Asia*, **7**, 121 (2003); (b) S.A. Chavan, D. Srinivas, P. Ratnasamy. *J. Catal.*, **204**, 409 (2001); (c) S.A. Chavan, D. Srinivas, P. Ratnasamy. *J. Catal.*, **212**, 39 (2002).

[12] C. Bowers, P.K. Dutta. *J. Catal.*, **122**, 271 (1990).

[13] P.K. Dutta, M. Ledney. *Prog. Inorg. Chem.*, **44**, 209 (1997).

[14] D. Kaucky, A. Vondrova, J. Dedecek, B. Wichterlova. *J. Catal.*, **194**, 318 (2000).

[15] E.F. Sousa-Aguiar, C.J.A. Mota, M.L.M. Valle, M.P. Silva, D.F. Silva. *J. Mol. Catal. A: Chem.*, **104**, 267 (1996).

[16] E.F. Sousa-Aguiar, M.L.M. Valle, M.P. Silva, D.F. Silva. *Zeolites*, **15**, 620 (1995).

[17] J. Basset, G.H. Denney, G.H. Jeffery, J. Mendham. *Vogel's Textbook of Quantitative Inorganic Analysis*, p. 429, Wiley, New York (1987).

[18] S.W. Wang, H. Everett, R.A.W. Haul, L. Moscou, R.A. Pierotti, J. Rouquerol, T. Siemieniewska. *Pure Appl. Chem.*, **57**, 603 (1985).

[19] A. Lineares-Solano. In *Carbon and Coal Gasification*, J.L. Figueiredo, J.A. Moulijn (Eds), p. 137, Martinus Nijhoff Publishers, Dordrecht (1986).

[20] S. Chandra, L.K. Gupta, D. Jain. *Spectrochim. Acta, Part A*, **60**, 2411 (2004).

[21] S. Chandra, K. Gupta. *Transition Met. Chem.*, **27**, 329 (2002).

[22] S. Chandra, L.K. Gupta. *J. Saudi Chem. Soc.*, **7**, 243 (2003).

[23] M. Shakir, S.P. Varkey, P.S. Hameed. *Polyhedron*, **12**, 2775 (1993).

[24] D.H. Cook, D.E. Fenton. *Inorg. Chim. Acta*, **25**, L95 (1977).

[25] M. Salavati-Niasari, M. Rezai-Adaryani. *Polyhedron*, **23**, 1325 (2004).

[26] M. Salavati-Niasari. *Polyhedron*, **24**, 1405 (2005).

[27] M. Salavati-Niasari, F. Davar. *Polyhedron*, **25**, 2127 (2006).

[28] G.A. Lawrence, M.A. O'Leary. *Polyherdon*, **6**, 1291 (1987).

[29] M.P. Suh, W. Shin, D. Kim, S. Kim. *Inorg. Chem.*, **23**, 618 (1984).

[30] G. Pattrick, M.P. Ngwenya, S.M. Dobson, R.D. Hancock. *J. Chem. Soc., Dalton Trans.*, 1295 (1991).
[31] R.D. Hancock. *Acc. Chem. Res.*, **23**, 253 (1990).
[32] T.W. Hambley, G.A. Lawrence, M. Maeder, E.N. Wikes. *J. Chem. Soc., Dalton Trans.*, 1283 (1992).
[33] P.V. Bernhart, G.A. Lawrence. *Coord. Chem. Rev.*, **93**, 297 (1990).
[34] R.W. Hay, B. Jeragh, G. Ferguson, B. Kaiter, B.L. Rule. *J. Chem. Soc., Dalton Trans.*, 1531 (1982).
[35] R.W. Hay, D.P. Piplani. *J. Chem. Soc., Dalton Trans.*, 1956 (1977).
[36] L. Fabbrizzi. *Inorg. Chem.*, **18**, 438 (1977).
[37] M.P. Suh, B.Y. Shim, T.-S. Yoon. *Inorg. Chem.*, **33**, 5509 (1994).
[38] B.J. Hathaway. In *Comprehensive Coordination Chemistry*, Sir G. Wilkinson, G.D. Gillard, J.A. McCleverty (Eds), Vol. 5, Chap. 53, p. 533, Pergamon Press, Oxford (1987).
[39] F.V. Lovecchio, E.S. Gore, D.H. Busch. *J. Am. Chem. Soc.*, **96**, 3109 (1974).
[40] M. Salavati-Niasari, F. Davar. *Inorg. Chem. Commun.*, **9**, 175 (2006).
[41] M.P. Suh, S.-G. Kang. *Inorg. Chem.*, **27**, 2544 (1988).
[42] E.K. Barefield. *Inorg. Chem.*, **11**, 2273 (1972).
[43] M. Salavati-Niasari. *Inorg. Chem. Commun.*, **8**, 174 (2005).
[44] M. Salavati-Niasari. *J. Mol. Catal. A: Chem.*, **245**, 192 (2006).
[45] M. Salavati-Niasari. *J. Mol. Catal. A: Chem.*, **284**, 97 (2008).
[46] T.H. Bennur, D. Srinivas, S. Sivasanker. *J. Mol. Catal. A: Chem.*, **207**, 163 (2004).